

BMC Biology 5:18 (2007).

Global and regional brain metabolic scaling and its functional consequences

Jan Karbowski

Sloan-Swartz Center for Theoretical Neurobiology,

Division of Biology 216-76,

California Institute of Technology, Pasadena, CA 91125, USA

Abstract

Background: Information processing in the brain requires large amounts of metabolic energy, the spatial distribution of which is highly heterogeneous reflecting complex activity patterns in the mammalian brain.

Results: Here, it is found based on empirical data that, despite this heterogeneity, the volume-specific cerebral glucose metabolic rate of many different brain structures scales with brain volume with almost the same exponent around -0.15 . The exception is white matter, the metabolism of which seems to scale with a standard specific exponent $-1/4$. The scaling exponents for the total oxygen and glucose consumptions in the brain in relation to its volume are identical and equal to 0.86 ± 0.03 , which is significantly larger than the exponents $3/4$ and $2/3$ suggested for whole body basal metabolism on body mass.

Conclusions: These findings show explicitly that in mammals (i) volume-specific scaling exponents of the cerebral energy expenditure in different brain parts are approximately constant (except brain stem structures), and (ii) the total cerebral metabolic exponent against brain volume is greater than the much-cited Kleiber's $3/4$ exponent.

The neurophysiological factors that might account for the regional uniformity of the exponents and for the excessive scaling of the total brain metabolism are discussed, along with the relationship between brain metabolic scaling and computation.

Keywords: Brain metabolism, allometric scaling, neurophysiology, brain design, whole-body metabolism, Kleiber's law.

email: jkarb@its.caltech.edu

Background

The brain is one of the most expensive tissues in the body [1, 2, 3], as it uses large amounts of metabolic energy for information processing [4, 5, 6, 7]. Because of this, neural codes are constrained not only by a combination of structural and functional requirements [8, 9, 10, 11, 12, 13, 14, 15, 16, 17], but also by energetic demands [6, 7, 18, 19, 20, 21]. In general, it has been observed that an elevated synaptic signaling between neurons leads to more energy consumed [22], which is used in imaging experiments [23]. Although some theoretical progress has been made in quantifying contributions of different neurophysiological processes to the total metabolic expenditure of a single neuron [20], the metabolism of large-scale neural circuits has not been investigated quantitatively. Here, a first step in this direction is made by studying global and regional *in vivo* brain metabolic scaling. There is a long tradition in applying allometric scaling to problems in biology [1], in particular to whole body metabolism [1, 24], but surprisingly not to cerebral metabolism. The goal of this paper is to find, by collecting and analyzing data, scaling metabolic exponents of different parts of the brain, as well as its global exponent. It is found that the volume-specific exponents across cerebral regions on brain volume are almost identical, approximately -0.15 . Consequently, the energy consumption of the entire brain tissue scales with brain volume with the exponent ≈ 0.86 . The main neurophysiological factors that might cause the increase of the latter exponent well above the putative Kleiber's $3/4$ scaling exponent characterizing whole-body energy expenditure on body mass [24], are identified. The consequences of brain metabolic scaling on its information processing capacity in the context of brain

design are also discussed.

Results

Oxygen and glucose are the main components involved in the production of ATP, which is used in cellular energetics [3, 4, 6], and therefore their rates of utilization provide useful measures of brain metabolism. There are several mammalian species, spanning more than 3 orders of magnitude in brain size, for which *in vivo* brain metabolic data are available (see Materials and Methods). The allometric laws characterizing global cerebral metabolism of oxygen and glucose are similar and yield an identical scaling exponent 0.86 ± 0.03 against brain volume (Fig. 1). It is important to note that this value is significantly larger ($p \leq 0.05$) than the exponents $3/4$ [1, 24] and $2/3$ [25] found for whole body mammalian metabolism in relation to body mass.

The cerebral cortex is a critical part of the brain responsible for integrating sensory information, and commanding behavioral and cognitive tasks. Regions of the cerebral cortex differ both in molecular detail and in biological function, which is manifested in a non-uniform distribution of neuronal activity and energy utilization throughout the cortex [5] (and Supplementary Information). However, despite this heterogeneity values of the scaling exponents of the regional volume-specific glucose utilization rates on brain volume (CMR_{glc} ; glucose cerebral metabolic rate per brain region volume) are surprisingly homogeneous; they are either exactly equal to -0.15 or are close to this value (Fig. 2 and Table 1). Consequently, also the average specific glucose utilization rate of the whole cerebral cortex scales with the exponent -0.15 ± 0.03 with brain

volume (Fig. 2E), which is equivalent to the exponent 0.85 ± 0.03 for the metabolism of the entire cortical volume; the value close to that for the whole brain (Fig. 1).

Some subcortical structures of gray matter utilize half of the energy used in the cortex (e.g., limbic structures in cat and monkey; see Clarke and Sokoloff [5] and Supplementary Information), and yet almost all of them exhibit a similar scaling homogeneity, with metabolic specific exponents also around -0.15 (Fig. 3, and Table 1). Volume-specific metabolisms of two brain stem structures - superior colliculus (involved in visual coordination) and inferior colliculus (involved in auditory processing) - seem to be exceptions, since they scale with brain size with the exponent ≈ 0 (Table 1). This might be caused by their highly variable activities (see Supplementary Information), and we do not know how other brain stem structures behave. The high degree of allometric uniformity for the most of the subcortical system is even more striking than that for the cortex, since subcortical regions are much more diverse in function and biophysical properties than cortical areas. For example, thalamus and hippocampus play extremely different roles in the brain, the former mediating sensory input to the cortex, while the latter implicated in memory processes, and still their scaling exponents and corresponding confidence intervals are almost identical (Figs. 3A,B, and Table 1).

Metabolism of white matter is about three-fold lower than that of gray matter [4, 5], and the results in Table 1 indicate that also their scaling exponents might differ. Specific glucose metabolisms of the two main structures of white matter, corpus callosum and internal capsule, scale similarly with brain volume with the average exponent around $-1/4$ (Fig. 4, Table 1). This value resembles the whole body specific metabolic

exponent against body mass.

Discussion

General discussion.

The total metabolic exponent 0.86 ± 0.03 , found for unanesthetized mammalian brains, implies that cerebral energy use increases more steeply with brain size than does whole body energy use with body size. This might be a reason why brain size increases slower than its body size, with the power $3/4$ [26]. However, the metabolic exponent 0.86 undermines Martin's [26, 27] well-known argument that the $3/4$ scaling of brain size reflects allometric isometry between brain metabolic needs and its size (exponent 1). Instead, the product of the exponents for brain size on body size and brain metabolic rate on brain size gives an exponent for brain metabolic needs on body size of about 0.65, which is lower than 0.75, expected from the assumption of isometry. Thus, depending on the scaling reference the total brain metabolism scales either above the Kleiber's $3/4$ power if in relation to brain mass, or below the Kleiber's power if in relation to body mass.

The discovered uniformity, i.e. constancy, of the cerebral specific exponents in gray matter suggests a common principle underlying basal metabolism of different brain structures, which might be associated with the homogeneity of synaptic density throughout the gray matter [28, 29]; see below.

In analyzing comparative allometry some authors use phylogenetic approaches in or-

der to include dependencies in data sets [30, 31]. However, these sophisticated methods require as a prerequisite the knowledge of a phylogenetic tree and associated branching parameters for species of interest. This is not a trivial matter to do, and therefore not applied in the present analysis. Also, because correlations in most scaling plots (Figs. 1-4, Table 1) are generally very high, it is likely that taking phylogeny into account would not alter the empirical exponents.

Key factors in the cerebral metabolic rate.

Which factors in the gray matter might account for its total metabolic exponent on brain volume greater than 3/4? The likely candidate is the density of glial cells, which provide metabolic support for neurons (including synapses) [32, 33]. Two recent studies [34, 35] show that the number of glia per neuron increases for larger brains, suggesting that neurons become more energy expensive with increasing brain size. In particular, the total number of glia in the cerebral cortex of rodents scales with brain size with the exponent 0.89 (Fig. 2B in [34]), which is close to the empirical metabolic exponent 0.86. It is likely that glia number simply follows energetic demands of neurons, especially their spatial expansion with increasing brain size. Thus, the details of this expansion may provide clue about which neural factor are important.

It has been estimated that neural metabolism is dominated by Na^+/K^+ -ATPase ion transport [6, 36, 37, 38]. The bulk of this comes from active ion fluxes at synapses and along axon (propagation of axon potentials) if neural firing rate is sufficiently large [20]. The synaptic contribution in a single neuron is proportional to the product of the

number of synapses per neuron, firing rate, release probability, and the postsynaptic charge. The active axon contribution is proportional to its surface area and firing rate. When neurons do not fire action potentials they also consume energy, because of the passive Na^+ and K^+ ion flow that electro-chemical Na^+/K^+ pump must remove to maintain their gradients across the membrane [39]. This resting potential contribution is proportional to the total neuron's surface area. To obtain the total cerebral energy consumption one has to multiply all these three additive contributions by the total number of neurons in the gray matter.

It seems that from all these three neural contributions the most dramatic for the scaling exponent of the total brain metabolism on brain volume is the synaptic contribution. This contribution is proportional to the total number of synapses in the gray matter, which scales with the gray matter volume, and thus brain volume [40, 41], with the exponent 1. This follows from regional- and scale-invariance of synaptic density [28, 29]. The regional homogeneity of synaptic density correlates with the discovered homogeneity of the regional volume-specific cerebral metabolic scaling (Table 1). Moreover, if remaining factors comprising the synaptic contribution, i.e., firing rate, release probability, and postsynaptic charge were brain size independent, then the synaptically driven total brain metabolism would scale with brain volume with the exponent 1. Since this exponent is, in fact, between 3/4 and 1 (Fig. 1), it implies that either of these 3 factors (or all of them) decrease with brain size. It could be hypothesized that because synaptic sizes and their basic molecular machinery are similar among mammals of different sizes [28, 39], the postsynaptic component might be roughly the same among

different species. This suggests that the product of the firing rate and release probability should decrease as brains increase in size, with a power of about -0.15 , which is in accord with low firing rates in humans estimated based on their basal cerebral metabolic rate [21, 42]. This also suggests that the number of active synapses in the background state decreases for bigger brains. That firing rate should decrease with brain (body) size is also consistent with allometric data of avian sensory neurons firing rates [43].

The remaining two contributions affecting metabolic rate, the active axons and maintaining the resting potentials, are both proportional to the product of the number of neurons in the gray matter and axonal surface area (assuming that axon surface area constitutes the majority of the neuron's area, especially for bigger brains). Additionally, the active axon contribution is proportional to the average firing rate. Given the above indications that the firing rate likely decreases with brain volume the active axon contribution becomes less important for the total metabolic exponent as brains increase in size. Thus, we focus only on the resting potential contribution. Since the product of the number of neurons and axonal surface area is proportional to the ratio of the volume of gray matter to axon diameter (due to the empirical fact that volumes of intracortical axons and gray matter are proportional across species [28]), the resting potential contribution produces the total metabolic exponent that is determined by the scaling exponent of the axon diameter against brain volume. The bigger the axonal exponent, the smaller the metabolic exponent. There are some sketchy experimental indications that axon diameter indeed increases with brain size [44, 45], e.g., in the corpus callosum with the exponent ≈ 0.07 [44]. If similar allometry holds for the gray

matter axons, the resting potential contribution would yield a total metabolic exponent also above $3/4$.

Brain metabolism, computation, and design.

The facts that the synaptic metabolic contribution decreases with decreasing the rate of release probability, and that the active axon and resting potential metabolic contributions decrease with increasing axon diameter have interesting functional consequences. Higher failure rate of synaptic transmission as brains get bigger not only saves energy but it also may maximize information transfer to postsynaptic neurons [19]. Similarly, increasing axon diameter with brain size accomplishes three functions simultaneously: it reduces the specific metabolic rate, increases the number of synapses per neuron, and it increases the speed of signal propagation in cortical circuits, which is proportional to the square root of the axon diameter [46, 47]. It is difficult to say at this stage whether these relationships are accidental or maybe a result of some cerebral optimization.

We can estimate the allometric cost of information processing by finding how the amounts of metabolic energy per neuron and per synapse scale with brain size. Since the total energy utilized by the entire cerebral cortex (gray matter) scales with its volume V_g with the exponent ≈ 0.85 (Table 1, Fig. 2E), the cerebral energy per neuron is $\propto V_g^{0.85}/(\rho_n V_g) \propto V_g^{0.05-0.17}$, i.e., it increases with brain size, where we used the fact that the neural density ρ_n scales with brain volume with the exponent between -0.32 and -0.20 (based on data of Haug (1987) [48]; see Supplementary Fig. S2). This in-

crease is in accord with the trend of increasing the number of glial cells per neuron in gray matter. The opposite is true for synapses, since the energy per synapse is $\propto V_g^{0.85}/(\rho_s V_g) \propto V_g^{-0.15}$, where ρ_s is the synaptic density (independent of brain size). The increase in energy expenditure per neuron with increasing brain size is in contrast to findings in liver cells [49], whose metabolism decreases with body mass. This difference reflects the increase of neural size (its wire) and corresponding decrease in density with increasing brain volume (sizes of liver cells are roughly constant [50]). The decaying trend for synapses implies again that their active fraction decreases as brains get bigger. These results have implications for coding and cortical organization. The fact that expanding neurons are energetically costly was probably a driving evolutionary force in decreasing their density in larger mammals (Supplementary Fig. S2) and adopting sparse neural representations [18, 20, 21]. The latter factor is consistent with the idea of functional modularity of the cerebral cortex [40], i.e., that primary information processing takes place in local modules/areas. The sizes of such modules/areas seem to follow scaling rules [12, 15, 40], and have been shown to have almost brain size independent connectedness [12] as opposed to neural connectedness that decays with brain size [11, 12].

Metabolism of gray versus white matter.

The data in Table 1 seem to indicate that the white matter and gray matter metabolic allometries are different. This finding implies that as brains increase in size, the white matter metabolism is less costly than that of gray matter. This is presum-

ably beneficial for the total cerebral energetic expenditure, since white matter increases disproportionately faster than gray matter [9, 40, 51]. The difference in white and gray matter metabolisms may be caused by their apparent neuroanatomical differences, since most of the white matter axonal membrane is covered with myelin sheath, which prevents ions flow and reduces metabolic cost.

Relation to metabolism of other tissues.

Most of the tissues in the body have much lower specific metabolic rate than the brain, with the exception of four highly active organs: kidney, liver, heart [1] and gut [2]. There exists no reliable data on *in vivo* allometric metabolic scaling in these tissues across different species (see however [52], where allometric exponents are given based on only 2-3 species). Allometric *in vitro* studies of Na^+/K^+ -ATPase in kidney [53] and in brain [54] suggest that these two organs might have comparable specific metabolic exponents. We can indirectly estimate and compare metabolic exponents for active tissues using allometric data on mitochondria size [55], since its total membrane surface area correlates with a baseline oxygen consumption [55]. (Interestingly, the total mitochondrial volume in locomotory muscles is proportional to the maximal metabolic rate in mammals [56].) We find that the total mitochondrial surface area in brain scales with brain mass with the exponent 0.86, i.e., exactly the same as that in Fig. 1. The corresponding scaling exponents for kidney, liver, and heart, against their respective organ masses are smaller and closer to the 3/4 exponent: 0.71, 0.74, and 0.81. These exponents do not seem to relate directly to the exponents of sizes of these tissues on body

size, since masses of kidney and liver increase slower than body mass, while heart mass scales isometrically [1]. Thus, it appears that, in general, higher metabolic exponents do not necessarily lead to lower mass exponents.

If these exponents reflect a real difference of metabolic allometry between cerebral and non-cerebral tissues, it might be caused by differences in membrane chemical composition and ion pump activities, which is known as the “membrane pacemaker theory of metabolism” [38]. For example, it has been shown that heart, liver, kidney, and skeletal muscles display allometric variation in lipid composition but brain does not [57]. Other potential factors (some of which might be related to the membrane pacemaker hypothesis) affecting differences in the allometries of brain and other tissues include: (i) distinct ways energy is utilized in the brain and in other tissues (e.g., Na^+/K^+ -ATPase dominates energy consumption only in the brain and kidney [3]); (ii) difference in a mode of activity (cells outside nervous system exhibit graded electrical activity without firing Na^+ action potentials); (iii) structural differences between brain and other highly active tissues (the size of non-cerebral cells is virtually independent of the body mass and the cells lack elongated processes with synapses, e.g., [50]); (iv) the existence of the blood-brain barrier that restricts a direct transport of molecules between bloodstream and nerve cells [39], which might affect substrate utilization rate and/or neural activity [58, 59].

Supply-limited models of metabolic scaling.

In many studies of whole body metabolism the scaling exponent $3/4$ was found [1,

24], and it was argued that this value follows from a general model of hierarchical fractal-like transport networks [60], or from constrained geometric networks with balanced supply and demand [61]. Both of these models are based on the assumption that metabolic rates are determined solely by resources supply rates and are independent of the cellular energy expenditure. This single-cause assumption has been challenged recently [62, 63]. The main arguments against the above supply-limited models are that (i) blood flow rate adjusts itself to tissue physiological demands and in resting animals is well below its maximal limit, and (ii) cellular metabolic rates decline with increasing body size [49] (at least for non-cerebral cells). Because of these facts a “multiple-causes” scenario of metabolic scaling has been proposed [62, 63], which in essence argues that supply rate is only one of the factors and should be considered together with other factors characterizing utilization of cellular energy. The approach taken in this paper is similar in spirit, i.e., given that the total cerebral metabolic exponent is 0.86, simple supply-limited models are rejected as a possible explanation for brain metabolic scaling. Instead, the most energetically expensive cellular factors that are most likely to affect the metabolic exponent were identified. In this sense, this approach can also be viewed as a multiple-cause model of the cerebral metabolic scaling.

Conclusions

Figures 1-3 and Table 1 provide an empirical evidence that the scaling exponents describing global and regional brain metabolism are significantly different ($p \leq 0.05$)

from the much-cited $3/4$ exponent, which calls into question the direct applicability of supply-limited models [60, 61] to brain metabolism. The exceptions are white matter structures, which seem to exhibit “regular” metabolic exponents (Fig. 4).

The empirical results presented in this paper show striking uniformity of the allometric metabolic exponents over almost entire gray matter of mammalian brains at normal resting conditions, despite anatomical and functional heterogeneity of different regions and their different levels of activation. This regional scaling uniformity is surprising, as activity level could potentially affect the scaling exponent. For example, the total metabolic rate of maximally exercised body scales with body mass well above $3/4$, with an exponent of 0.88 [56, 64].

Materials and Methods

In vivo data of the cerebral oxygen (CMR_{O_2}) and glucose (CMR_{glc}) utilization rates of unanesthetized adult animals at resting conditions were collected from different sources [65] (see Supplementary Information for details). In those studies the measurements of glucose utilization in all species were performed by essentially the same method or its modification (in human and baboon), and thus all glucose data are directly comparable. There is a small method variability for oxygen data, since the same technique was applied to five out of seven species (except cat and dog). However, this variability does not affect the scaling exponent (Fig. 1A) - it is exactly the same even if only single-method mammals are included in the plot. Glucose utilization data

represent both global and regional cerebral metabolism. The investigated mammals include: Swiss mouse (only glucose data), Sprague-Dawley rat, squirrel (only glucose data), rabbit (only glucose data), cat, dog (only oxygen data), macaque monkey, baboon, sheep, goat (only glucose data), and human. The investigated brain structures include: cerebral cortex (visual, prefrontal, frontal, sensorimotor, parietal, temporal, cingulate, occipital), thalamus (including lateral geniculate nucleus and medial geniculate nucleus), hypothalamus (and separately mammillary body), cerebellum (including cerebellar cortex and dentate nucleus), basal ganglia (caudate, substantia nigra, globus pallidus), limbic system (hippocampus, amygdala, septum), brain stem (superior colliculus, inferior colliculus), and white matter (corpus callosum, internal capsule). In the cases when there are more than one data point for a given animal or a brain structure, an arithmetic mean of all values was taken.

Allometric metabolism of the entire cerebral cortex, presented in Fig. 2E, was obtained by computing an arithmetic mean of glucose utilization in 8 cortical areas (listed above) for each animal. Glucose utilization of a given area was itself an average of values taken from different sources. If data for all 8 areas were not available, averaging was performed over lesser number of areas. For consistency, also an alternative method of averaging was used: first averaging was performed for a given source data, and second among different sources representing the same animal. In this method, because various sources differ in the number of cortical areas studied, averaging in many cases was performed over significantly different number of areas. However, both methods give statistically identical scaling exponents for the cerebral cortex metabolism (see Fig. S1

in Supplementary Information).

Allometric metabolism of the entire brain was obtained by using either direct data quoted by authors, or, if not available, by computing an arithmetic mean of glucose consumption in all brain structures provided by the authors. For all scaling plots brain volumes were taken from Hofman (1988) [41] and Stephan et al (1981) [66], or from the source.

Acknowledgments

The work was supported by the Sloan-Swartz Fellowship and by the Caltech Center for Biological Circuit Design.

References

- [1] Schmidt-Nielsen K (1984) *Scaling: Why is Animal Size so Important?* Cambridge: Cambridge Univ. Press.
- [2] Aiello LC, Wheeler P (1995) The expensive-tissue hypothesis: the brain and the digestive-system in human and primate evolution. *Curr. Anthropol.* **36**, 199-221.
- [3] Rolfe DFS, Brown GC (1997) Cellular energy utilization and molecular origin of standard metabolic rate in mammals. *Physiol. Rev.* **77**: 731-

758.

- [4] Siesjö B (1978) *Brain Energy Metabolism*. New York: Wiley.
- [5] Clarke DD, Sokoloff L (1994) In *Basic Neurochemistry*. Eds: G.J. Siegel et al (New York: Raven Press), pp. 645-680.
- [6] Ames A. 3rd (2000) CNS energy metabolism as related to function. *Brain Res. Rev.* **34**: 42-68.
- [7] Laughlin SB, de Ruyter van Steveninck RR, Anderson JC (1998) The metabolic cost of neural information. *Nature Neurosci.* **1**, 36-41.
- [8] Finlay BL, Darlington RB (1995) Linked regularities in the development and evolution of mammalian brains. *Science* **268**: 1578-1584.
- [9] Barton RA, Harvey PH (2000) Mosaic evolution of brain structure in mammals. *Nature* **405**: 1055-1058.
- [10] Clark DA, Mitra PP, Wang SSH (2001) Scalable architecture in mammalian brains. *Nature* **411**: 189-193.
- [11] Karbowski J (2001) Optimal wiring principle and plateaus in the degree of separation for cortical neurons. *Phys. Rev. Lett.* **86**: 3674-3677.
- [12] Karbowski J (2003) How does connectivity between cortical areas depend on brain size? Implications for efficient computation. *J. Comput. Neurosci.* **15**: 347-356.

- [13] Stevens CF (2001) An evolutionary scaling law for the primate visual system and its basis in cortical function. *Nature* **411**: 193-195.
- [14] Chklovskii DB, Schikorski T, Stevens CF (2002) Wiring optimization in cortical circuits. *Neuron* **34**: 341-347.
- [15] Chklovskii DB (2004) Synaptic connectivity and neural morphology: two sides of the same coin. *Neuron* **43**: 1-20.
- [16] Sporns O, Chialvo DR, Kaiser M, Hilgetag CC (2004) Organization, development and function of complex brain networks. *Trends Cogn. Sci.* **8**: 418-425.
- [17] Striedter GF (2005) *Principles of brain evolution*. Sunderland, MA: Sinauer Assoc.
- [18] Levy WB, Baxter RA (1996) Energy efficient neural codes. *Neural Comput.* **8**: 531-543.
- [19] Levy WB, Baxter RA (2002) Energy-efficient neuronal computation via quantal synaptic failures. *J. Neurosci.* **22**: 4746-4755.
- [20] Attwell D, Laughlin SB (2001) An energy budget for signaling in the grey matter of the brain. *J. Cereb. Blood Flow Metab.* **21**: 1133-1145.
- [21] Lennie P (2003) The cost of cortical computation. *Curr. Biol.* **13**: 493-497.

- [22] Sibson NR et al. (1998) Stoichiometric coupling of brain glucose metabolism and glutamatergic neuronal activity. *Proc. Natl. Acad. Sci. USA* **95**: 316-321.
- [23] Vanzetta I, Grinvald A (1999) Increased cortical oxidative metabolism due to sensory stimulation: Implications for functional brain imaging. *Science* **286**: 1555-1558.
- [24] Kleiber M (1932) Body size and metabolism. *Hilgardia* **6**: 315-353.
- [25] White CR, Seymour RS (2003) Mammalian basal metabolic rate is proportional to body mass^{2/3}. *Proc. Natl. Acad. Sci. USA* **100**: 4046-4049.
- [26] Martin RD (1981) Relative brain size and basal metabolic rate in terrestrial vertebrates. *Nature* **293**: 57-60.
- [27] Martin RD (1996) Scaling of the mammalian: The maternal energy hypothesis. *News in Physiological Sciences* **11**: 149-156.
- [28] Braitenberg V, Schüz A (1998) *Cortex: Statistics and Geometry of Neural Connectivity*. Berlin: Springer-Verlag.
- [29] Cragg BG (1967) The density of synapses and neurones in the motor and visual areas of the cerebral cortex. *J. Anatomy* **101**: 639-654.
- [30] Harvey PH, Pagel M (1991) *The comparative method in evolutionary biology*. Oxford: Oxford University Press.

- [31] Garland T, Bennett AF, Rezende EL (2005) Phylogenetic approaches in comparative physiology. *J. Exp. Biol.* **208**: 3015-3035.
- [32] Tsacopoulos M, Magistretti PJ (1996) Metabolic coupling between glia and neurons. *J. Neurosci.* **16**: 877-885.
- [33] Magistretti PJ (2006) Neuron-glia metabolic coupling and plasticity. *J. Exp. Biol.* **209**: 2304-2311.
- [34] Herculano-Houzel S et al (2006) Cellular scaling rules for rodent brains. *Proc. Natl. Acad. Sci. USA* **103**: 12138-12143.
- [35] Sherwood CC et al (2006) Evolution of increased glia-neuron ratios in the human frontal cortex. *Proc. Natl. Acad. Sci. USA* **103**: 13606-13611.
- [36] Astrup J, Sorensen PM, and Sorensen HR (1981) Oxygen and glucose consumption related to Na^+ - K^+ transport in canine brain. *Stroke* **12**: 726-730.
- [37] Erecinska M, Silver IA (1989) ATP and brain function. *J. Cereb. Blood Flow Metab.* **9**: 2-19.
- [38] Hulbert AJ, Else PL (2000) Mechanisms underlying the cost of living in animals. *Annu. Rev. Physiol.* **62**: 207-235.
- [39] Kandel ER, Schwartz JH, Jessell TM (1991) *Principles of Neural Science*. Norwalk, Connecticut: Appleton and Lange, 3rd edition.

- [40] Prothero JW (1997) Cortical scaling in mammals: A repeating units model. *J. Brain Res.* **38**: 195-207.
- [41] Hofman MA (1988) Size and shape of the cerebral cortex in mammals. II. The cortical volume. *Brain Behav. Evol.* **32**: 17-26.
- [42] Shoham S, O'Connor DH, Segev R (2006) How silent is the brain: is there a “dark matter” problem in neuroscience? *J. Comp. Physiol. A* **192**: 777-784.
- [43] Hempleman SC, et al (2005) Spike firing allometry in avian intrapulmonary chemoreceptors: matching neural code to body size. *J. Exp. Biol.* **208**: 3065-3073.
- [44] Olivares R, Montiel J, Aboitiz F (2001) Species differences and similarities in the fine structure of the mammalian corpus callosum. *Brain Behav. Evol.* **57**: 98-105.
- [45] Harrison KH, Hof PR, Wang SSH (2002) Scaling laws in the mammalian neocortex: Does form provide clues to function? *J. Neurocytol.* **31**: 289-298.
- [46] Hodgkin AL (1954) A note on conduction velocity. *J. Physiol.* **125**: 221-224.
- [47] Koch C (1998) *Biophysics of computation*. Oxford: Oxford Univ. Press.

- [48] Haug H (1987) Brain sizes, surfaces, and neuronal sizes of the cortex cerebri: A stereological investigation of Man and his variability and a comparison with some mammals (primates, whales, marsupials, insectivores, and one elephant). *Am. J. Anatomy* **180**: 126-142.
- [49] Porter RK, Brand MD (1995) Cellular oxygen consumption depends on body mass. *Am. J. Physiol.* **269**: R226-R228.
- [50] Purves D (1988) *Body and Brain*. Cambridge, Massachusetts: Harvard Univ. Press.
- [51] Zhang K, Sejnowski TJ (2000) A universal scaling law between gray matter and white matter of cerebral cortex. *Proc. Natl. Acad. Sci. USA* **97**: 5621-5626.
- [52] Wang Z, O'Connor TP, Heshka S, Heymsfield SB (2001) The reconstruction of Kleiber's law at the organ-tissue level. *J. Nutr.* **131**: 2967-2970.
- [53] Turner N, Haga KL, Hulbert AJ, Else PL (2005a) Relationship between body size, $\text{Na}^+\text{-K}^+\text{-ATPase}$ activity, and membrane lipid composition in mammal and bird kidney. *Am. J. Physiol.* **288**: R301-R310.
- [54] Turner N, Else PL, Hulbert AJ (2005b) An allometric comparison of microsomal membrane lipid composition and sodium pump molecular activity in the brain of mammals and birds. *J. Exp. Biol.* **208**: 371-381.

- [55] Else PL, Hulbert AJ (1985) Mammals: an allometric study of metabolism at tissue and mitochondrial level. *Am. J. Physiol.* **248**: R415-R421.
- [56] Weibel ER and Hoppeler H (2005) Exercise-induced maximal metabolic rate scales with muscle aerobic capacity. *J. Exp. Biol.* **208**: 1635-1644.
- [57] Hulbert AJ, Else PL (2005) Membranes and the setting of energy demand. *J. Exp. Biol.* **208**: 1593-1599.
- [58] Devor A et al. (2003) Coupling of total hemoglobin concentration, oxygenation, and neural activity in rat somatosensory cortex. *Neuron* **39**: 353-359.
- [59] Sheth SA et al. (2004) Linear and nonlinear relationships between neural activity, oxygen metabolism, and hemodynamic responses. *Neuron* **42**: 347-355.
- [60] West GB, Brown JH, Enquist BJ (1997) A general model for the origin of allometric scaling laws in biology. *Science* **276**: 122-126.
- [61] Banavar JR, Damuth J, Maritan A, Rinaldo A (2002) Supply-demand balance and metabolic scaling. *Proc. Natl. Acad. USA* **99**: 10506-10509.
- [62] Darveau CA, Suarez RK, Andrews RD, Hochachka PW (2002) Allometric cascades as a unifying principle of body mass effects on metabolism. *Nature* **417**: 166-170.

- [63] Suarez RK, Darveau CA (2005) Multi-level regulation and metabolic scaling. *J. Exp. Biol.* **208**: 1627-1634.
- [64] Bishop CM (1999) The maximum oxygen consumption and aerobic scope of birds and mammals: getting to the heart of the matter. *Proc. R. Soc. B* **266**: 2275-2281.
- [65] Glucose utilization data were taken from: Bouilleret V et al., *Brain Res.* **852**, 255-262 (2000) and Quelven I et al., *Neurosci.* **126**, 441-449 (2004) for mouse; Dube C et al., *Exper. Neurol.* **167**, 227-241 (2001), Nehlig A et al., *J. Neurosci.* **8**, 2321-2333 (1988), Nehlig A and Boyet S, *Brain Res.* **858**, 71-77 (2000), Levant B and Pazdernik TL, *Brain Res.* **1003**, 159-167 (2004), Waschke K et al., *Am. J. Physiol.* **265**, H1243-H1248 (1993), Zocchi A et al., *Neurosci. Lett.* **306**, 177-180 (2001) and Blin J et al., *Brain Res.* **568**, 215-222 (1991) for rat; Passero S et al., *Neurosci. Lett.* **21**, 345-349 (1981) for rabbit; Frerichs KU et al., *Am. J. Physiol.* **268**, R445-R453 (1995) for squirrel; Chugani HT et al., *J. Cereb. Blood Flow Metabol.* **11**, 35-47 (1991), Schwartzman RJ, et al., *Brain Res.* **398**, 113-120 (1986), Sokoloff L, *Metabolic Probes of Central Nervous System Activity in Experimental Animals and Man*, (Sinauer, Sunderland, MA, 1984), Lydic R et al., *J. Comp. Neurol.* **304**, 517-529 (1991), and Herdman SJ et al., *J. Neurosci.* **9**, 1150-1162 (1989) for cat; Porrino LJ et al., *J. Neurosci.* **22**, 7687-7694 (2002), Palombo E et al., *J. Neurosci.* **10**, 860-869 (1990), Noda A et al., *Brain Res.*

936, 76-81 (2002) and Kennedy C et al., *Ann. Neurol* **4**, 293-301 (1978) for macaque monkey; Meguro K et al., *Brain* **122**, 1519-1531 (1999) for baboon; Pelligrino DA et al., *Am. J. Physiol.* **268**, R276-R283 (1987) for goat; Pell JM and Bergman EN *Am. J. Physiol.* **244**, E282-E289 (1983) for sheep (both glucose and oxygen); Blin J et al., *Brain Res.* **568**, 215-222 (1991), Maquet P et al., *Brain Res.* **571**, 149-153 (1992), Heiss WD et al., *Brain Res.* **327**, 362-366 (1985), Haier RJ et al., *Brain Res.* **570**, 134-143 (1992), Redies C et al., *Am. J. Physiol.* **256**, E805-E810 (1989), De Volder AG et al., *Brain Res.* **750**, 235-244 (1997), Blomqvist G et al., *Acta Physiol. Scand.* **163**, 403-415 (1998), and Clarke DD, Sokoloff L (1994), cited above, for human. Oxygen consumption data were taken from: Linde R et al., *Acta Physiol. Scand.* **165**, 395-401 (1999) for rat; Stingele R et al., *Am. J. Physiol.* **271**, H579-H587 (1996) for cat; Nakanishi O et al., *Can. J. Anaesth.* **44**, 1008-1013 (1997) for dog; Nemoto EM et al., *J. Neurosurg. Anesthesiol.* **6**, 170-174 (1994) for macaque monkey; Sahlin C et al., *Brain Res.* **403**, 313-332 (1987) for baboon; Madsen PL et al., *J. Appl. Physiol.* **70**, 2597-2601 (1991), and Clarke DD, Sokoloff L (1994), cited above, for human.

- [66] Stephan H, Baron G, Frahm HD (1981) New and revised data on volumes of brain structure in insectivores and primates. *Folia Primatol.* **35**: 1-29.

Table 1.

Specific scaling exponents of the regional cerebral glucose utilization rate CMR_{glc} against brain volume.

| Brain structure | Scaling exponent | 95% confidence intervals | Correlation R^2 (p -value) | Number of species |
|------------------------|------------------|--------------------------|---------------------------------|-------------------|
| <i>Cerebral cortex</i> | -0.15 ± 0.03 | $(-0.22, -0.08)$ | 0.870 (0.0022) | 7 |
| Visual | -0.12 ± 0.03 | $(-0.17, -0.08)$ | 0.932 (0.0018) | 6 |
| Prefrontal | -0.17 ± 0.03 | $(-0.23, -0.10)$ | 0.953 (0.0044) | 5 |
| Frontal | -0.14 ± 0.02 | $(-0.17, -0.12)$ | 0.997 (0.0015) | 4 |
| Sensorimotor | -0.15 ± 0.02 | $(-0.19, -0.11)$ | 0.945 (0.0002) | 7 |
| Parietal | -0.15 ± 0.03 | $(-0.20, -0.11)$ | 0.954 (0.0008) | 6 |
| Temporal | -0.15 ± 0.05 | $(-0.27, -0.03)$ | 0.680 (0.0224) | 7 |
| Cingulate | -0.16 ± 0.03 | $(-0.23, -0.09)$ | 0.912 (0.0030) | 6 |
| Occipital | -0.20 ± 0.12 | $(-0.53, 0.12)$ | 0.563 (0.1439) | 5 |
| <i>Thalamus</i> | -0.15 ± 0.03 | $(-0.22, -0.08)$ | 0.858 (0.0027) | 7 |
| <i>Hypothalamus</i> | -0.10 ± 0.04 | $(-0.20, -0.01)$ | 0.692 (0.0402) | 6 |
| Mammillary body | -0.15 ± 0.07 | $(-0.30, 0.00)$ | 0.773 (0.0495) | 5 |
| <i>Cerebellum</i> | -0.15 ± 0.04 | $(-0.24, -0.06)$ | 0.840 (0.0102) | 6 |
| <i>Basal ganglia</i> | | | | |
| Caudate | -0.15 ± 0.03 | $(-0.22, -0.08)$ | 0.905 (0.0035) | 6 |
| Substantia nigra | -0.14 ± 0.02 | $(-0.18, -0.10)$ | 0.956 (0.0007) | 6 |
| Globus pallidus | -0.16 ± 0.04 | $(-0.24, -0.08)$ | 0.926 (0.0088) | 5 |
| <i>Limbic system</i> | | | | |
| Hippocampus | -0.14 ± 0.03 | $(-0.19, -0.09)$ | 0.919 (0.0007) | 7 |
| Amygdala | -0.12 ± 0.03 | $(-0.17, -0.07)$ | 0.919 (0.0025) | 6 |
| Septum | -0.16 ± 0.03 | $(-0.23, -0.09)$ | 0.944 (0.0057) | 5 |
| <i>Brain stem</i> | | | | |
| Superior colliculus | -0.06 ± 0.05 | $(-0.19, 0.06)$ | 0.448 (0.2168) | 5 |
| Inferior colliculus | 0.05 ± 0.09 | $(-0.14, 0.23)$ | 0.174 (0.4843) | 5 |
| <i>White matter</i> | | | | |
| Corpus callosum | -0.23 ± 0.09 | $(-0.40, -0.06)$ | 0.947 (0.0271) | 4 |
| Internal capsule | -0.24 ± 0.12 | $(-0.48, 0.00)$ | 0.902 (0.0504) | 4 |

t-test shows that population mean of the exponents in the second column is significantly greater than the exponent -0.25 ($p = 9 \cdot 10^{-9}$, $\text{df}=21$ if white matter included; $p = 2 \cdot 10^{-9}$, $\text{df}=19$ if white matter excluded).

Figure Legends

Fig. 1

Scaling of the total basal cerebral metabolism with brain volume. The least-square fit line for the log-log plot yields: (A) For the total oxygen consumption rate the scaling exponent is 0.86 ± 0.04 ($y = 0.86x - 1.02$, $R^2 = 0.989$, $p < 10^{-4}$, $N = 7$), and its 95% confidence interval is (0.75, 0.96). (B) For the total glucose utilization rate an identical exponent 0.86 ± 0.03 is found ($y = 0.86x - 0.09$, $R^2 = 0.994$, $p < 10^{-4}$, $N = 10$), and its 95% confidence interval is (0.80, 0.91).

Fig. 2

Scaling of the cerebral cortex specific glucose utilization rate, CMR_{glc} , with brain volume. The specific metabolic scaling exponent, corresponding to the slope of the regression line, has the following values: (A) -0.12 for visual cortex ($y = -0.12x + 0.02$); (B) -0.15 for parietal cortex ($y = -0.15x + 0.01$); (C) -0.15 for sensorimotor cortex ($y = -0.15x + 0.02$); (D) -0.15 for temporal cortex ($y = -0.15x + 0.07$). (E) Average glucose utilization rate of the entire cerebral cortex yields the specific exponent -0.15 ($y = -0.15x + 0.03$).

Fig. 3

Scaling of the specific glucose utilization rate in subcortical gray matter with brain volume. The specific metabolic scaling exponent has the following values: (A) -0.15 for thalamus ($y = -0.15x + 0.03$); (B) -0.14 for hippocampus ($y = -0.14x - 0.13$), which represents limbic structures; (C) -0.15 for caudate ($y = -0.15x + 0.02$), which represents basal ganglia; (D) -0.15 for cerebellum ($y = -0.15x - 0.09$).

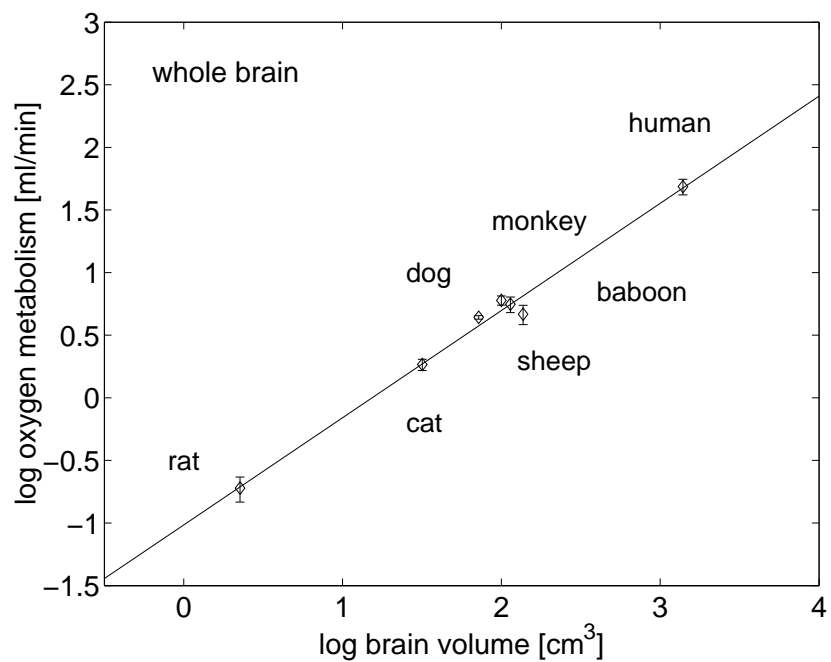
Fig. 4

Scaling of the volume-specific glucose utilization rate in white matter with brain volume.

(A) Corpus callosum metabolism yields the exponent -0.23 ($y = -0.23x - 0.45$), and

(B) internal capsule has a similar exponent -0.24 ($y = -0.24x - 0.41$).

A



B

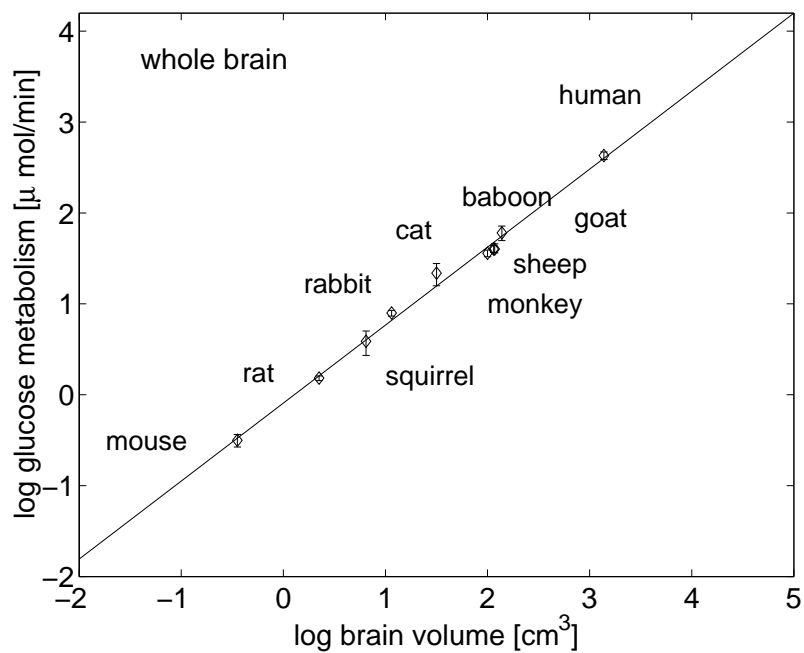


Figure 1

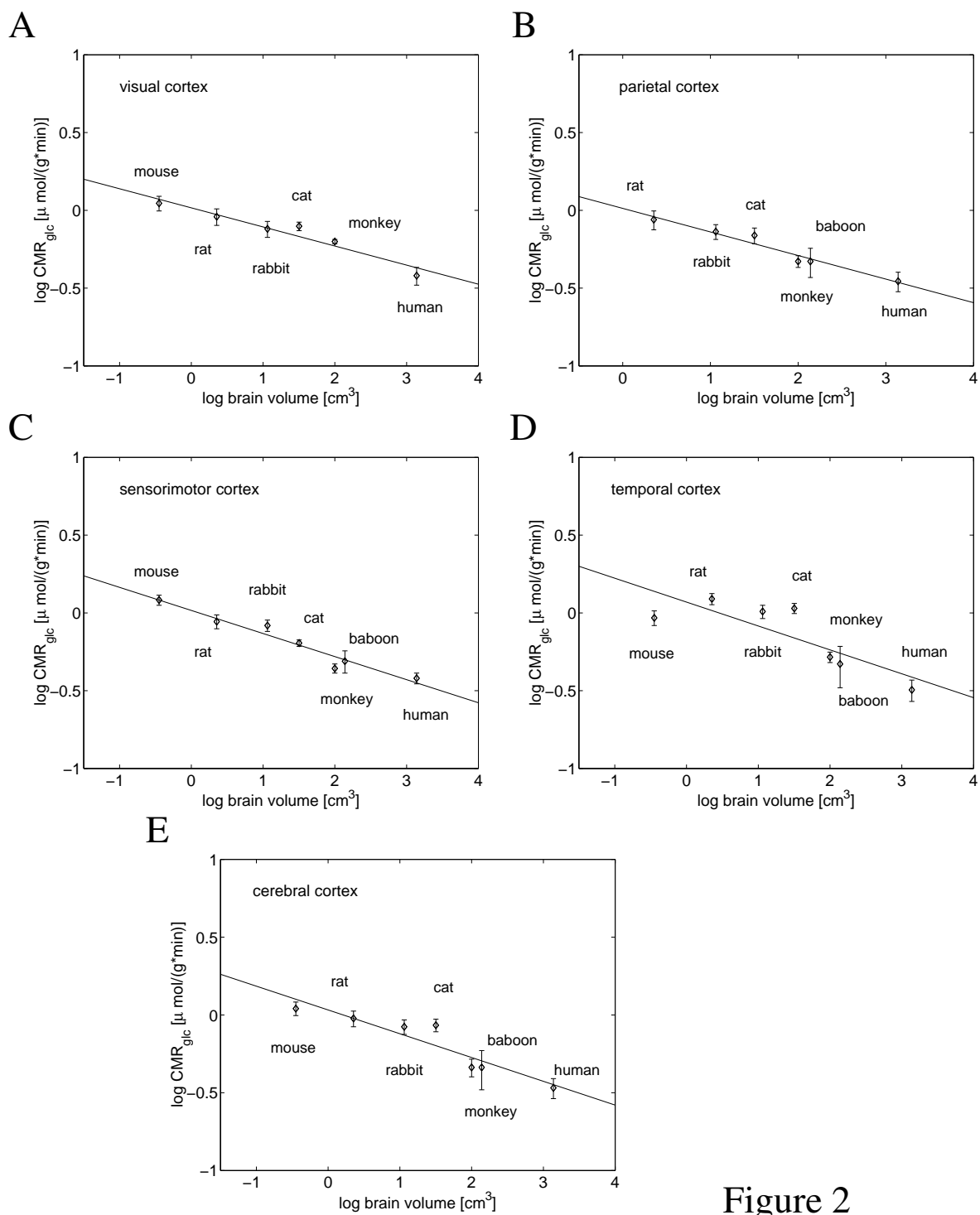


Figure 2

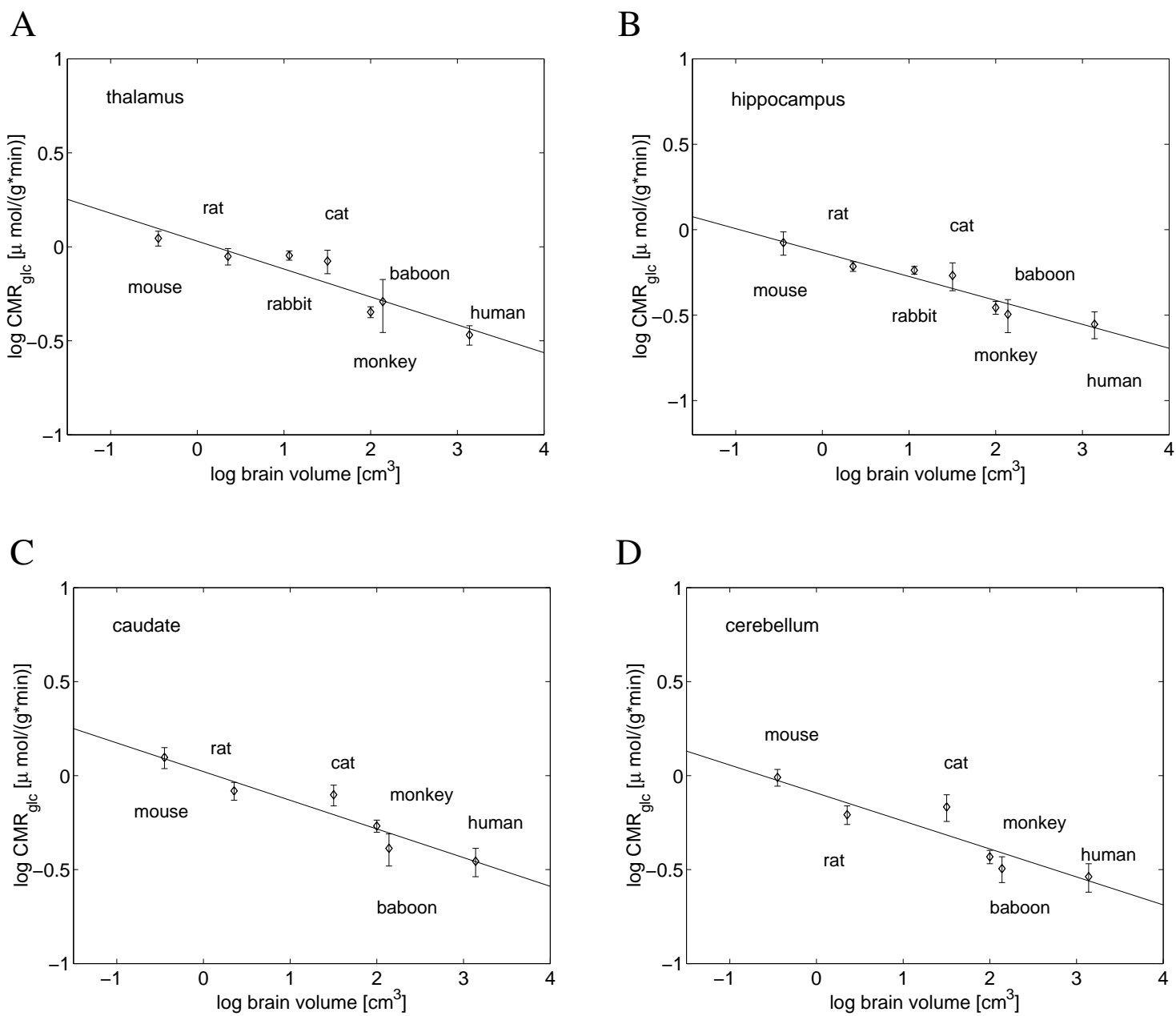
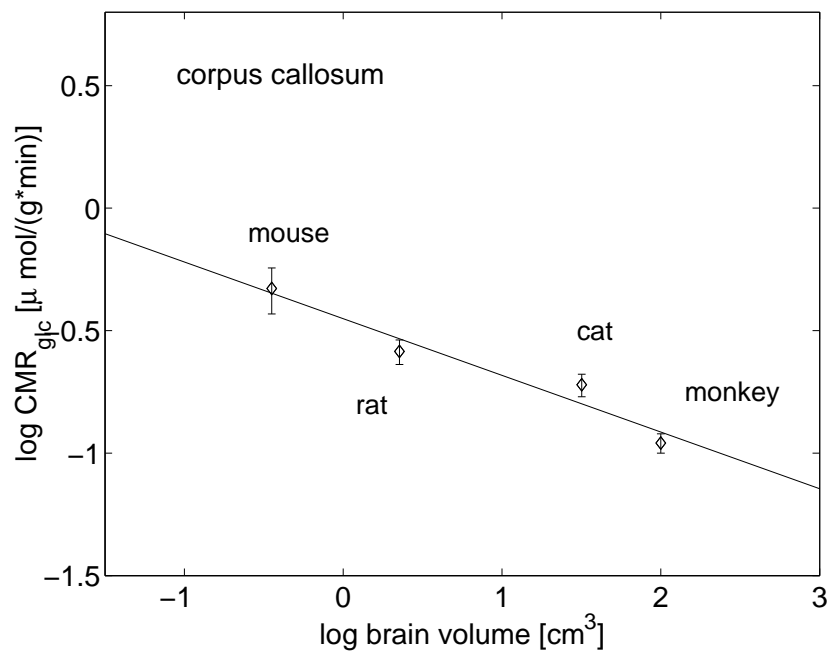


Figure 3

A



B

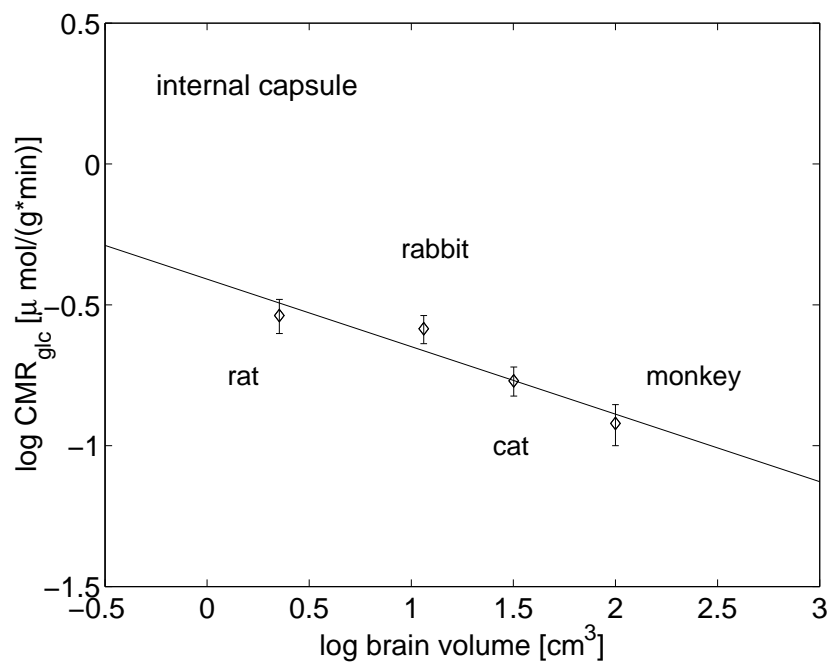


Figure 4